

NP Internal Report 69-2
14 February, 1969

A SUMMARY OF DISCUSSIONS ON
A LARGE MAGNETIC ANALYSIS SYSTEM OF ISR REACTIONS

by
K. Winter

THE UNIVERSITY OF CHICAGO
DEPARTMENT OF CHEMISTRY

1. INTRODUCTION

1.1 Purpose of the Project

There is general agreement that a large magnet system should be constructed at the ISR, which should provide the possibility of measuring the momenta of many charged reaction products in a geometry as nearly 4π as practicable. The system should be ready at the same time, or soon after, the ISR is available for experimentation, presumably by about the middle of 1971. It is likely that this will be the only large device capable of observing correlations between interaction products over at least some years; therefore it should be as generally useful as possible.

1.2 Purpose of this Report

This report summarizes information which could be useful in evaluating the merits of three different proposals. A list of references is given at the end. This information has been discussed and completed by a Working Group, which met 5 times. The members of this group were: B. French, B.D. Hyams, K. Johnsen (Chairman), F. Krienen, A. Michelini, A. Minten, B. de Raad, L. Resegotti, J. Steinberger and K. Winter (Secretary); the Director-General and the Chairman of the ISRC were guests.

Figures 1, 2 and 3 show the proposed magnet systems.

Comments and open questions, agreement and disagreement on the main problems, and also opinions are reported here. It is hoped that the report gives a faithful picture of people's views, and that it may help in deciding which magnet system is to be built. This attempt of an evaluation is organized in the following 5 chapters:

2. Acceptance
3. Event reconstruction
4. Detectors
5. Interference with ISR operation
6. Time schedule of construction.

2. ACCEPTANCE

A quantitative evaluation of acceptance, defined as the precision which can be achieved in the momentum measurement of reaction products as a function of their momenta and their (two) emission angles has been made⁴⁾. A comparison of the three proposed magnet systems was made under some assumptions which were applied uniformly to all three projects:

- a) A tube 15 cm in diameter centred on the beam.
- b) The detector cannot approach obstructions (magnet poles, beam tube) closer than 5 cm, so that particles cannot be detected at a radial distance of less than 12.5 cm from the beam centre.
- c) The detector is confined to the region of strong magnetic field $H > H_{\max}/2$.

A summary can be found in Tables 1 and 2 for positively and negatively charged particles, respectively. They give the fraction of the solid angle for secondaries with a sagitta > 2 cm for particles with momenta in the range 0.5 to 25 GeV/c and transverse momenta p_T up to 3 GeV/c. The averaged acceptances over these ranges of momenta and transverse momenta are given for all three systems. These global acceptances are of relevance for detection of high multiplicity events over a wide angular range.

The typical event may not be well approximated by an isotropic momentum and angle distribution. A better model may be a statistical distribution, given by the Coconci-Koester-Perkins formula. For pions one would expect:

$$\text{Pions: } \frac{d^2 N}{dp dp_t} = e^{-p^2/p_0^2} p_t e^{-p_t/p_{t_0}} .$$

Using for the parameters values obtained by Hagedorn

$$p_0 = \langle p \rangle = 1.77 \text{ GeV/c}$$

$$p_{t_0} = \frac{1}{2} \langle p_t \rangle = 0.17 \text{ GeV/c}$$

the following fractions will be observed with a sagitta > 2 cm

	H = 0	K	S
π^+	0.58	0.92	0.85
π^-	0.62	0.99	0.89
$\pi^+ + \pi^-$	0.60	0.955	0.87

For protons one would guess a flat momentum distribution between 6 and 25 GeV/c and

$$\text{Protons: } \frac{d^2 N}{dp dp_t} = p_t \cdot e^{-p_t/p_{t0}} .$$

Using $p_{t0} = \frac{1}{2} \langle p_t \rangle = 0.25$ GeV/c one finds the following fractions:

H = 0	K	S
0.47	0.48	0.71

Limitations due to compensation magnets and shims have not been taken into account in these acceptance calculations and may change these results.

Discussion

The assumed size of the beam pipe, 15 cm ϕ , and an extra 5 cm distance from it for detectors has been discussed. The standard vacuum pipe has elliptical cross section, 5 cm vertical and 15 cm horizontal diameter and 2.3 mm wall thickness.

Steinberger justified the assumption of 15 cm tube diameter. The beam tube must have thin walls to reduce multiple scattering of particles which traverse it. A rigid, thin-walled tube must have circular cross section. Its diameter is then given by the largest beam dimension for maximum intensity, and equals the horizontal size of the standard elliptical vacuum

chamber. French and Krienen discussed early use of the "Terwilliger scheme" which allows to reduce the horizontal beam size to 5 cm (by superimposing locally all momenta), and the tube to 6 cm diameter. French and Krienen summed up the advantages of this beam:

- 1) Acceptance of high-energy protons at lower transverse momenta in all three schemes (See Tables 3 and 4). The Krienen system with central field becomes more comparable to Steinberger's split field system.
- 2) Thinner wall (proportionally to the radius) and so less multiple scattering and nuclear interaction.
- 3) Better vertex reconstruction for neutral V's decaying inside the tube.

Johnsen, Hyams and Steinberger commented on the disadvantages of a magnet which requires the Terwilliger scheme:

- 1) Not available over the first 1-2 years.
- 2) Conflict with other users; in odd number intersection regions the beam blows up twice in the horizontal size.
- 3) Loss in luminosity by a factor of 4 to 5; this limits study of rare processes.
- 4) Three times higher pressure and beam-gas interaction rate in the crossing regions due to reduced pumping speed.
- 5) Interaction of beam tails with the walls and resulting background.
- 6) This magnet system being planned as the most advanced research possibility on the ISR should be able to run under all beam conditions.

Hyams commented on the particular field configuration chosen by Hyams-O'Neill. It was chosen to minimize the displacement of the circulating proton beam. But he agreed that it is poor in accepting secondaries, particularly because the downstream magnets are badly matched to the central field.

3. EVENT RECONSTRUCTION

Tracks as sampled by various detector arrangements (discussed under 4) have to be reconstructed and tracked through the magnetic field to the production vertex in the beam tube.

Three closely connected problems were discussed:

- 1) Influence of field inhomogeneities on computing time.
- 2) Precision of determining the production angles at the vertex from the observed track segments, and the
- 3) Influence of multiple scattering in crossing the beam tube.

B. French and J. Steinberger have discussed point 1) with Wind from NP division. Wind has devised a method, now currently in use, to determine the momenta of particles in arbitrary magnetic fields. Instead of storing a field map in the computer and integrating track segments through it, he now converts the field map into a tabulated function of five parameters, one being the momentum, the four others track parameters. The momentum of a particle is obtained by comparing its track parameters to the table. The method allows to compress field maps containing some 10^6 points into an array of some $10^3 - 10^4$ words. The parameters can be adapted to the particular experiment. Therefore, there is no predictable difference in computer time for event reconstruction in rather homogeneous fields (central and downstream field in H-O system) and less homogeneous fields (magnets with open sides, Krienen and Steinberger system). Hyams expressed doubts as to whether this problem is completely solved.

Winter discussed points 2) and 3) and reported on calculations done by members of his group. They have generated events $p p \rightarrow p N^*$ and tracked the charged secondaries through one of the systems $\rightarrow n + \pi^+$ (split field). New coordinates were chosen at random in three assumed detectors on each track: New tracks were fitted to these new coordinates and X^2 minimized by searching for a new vertex point. The following mass resolutions ΔM_1 were obtained for a detection precision $\sigma = 0.5$ mm.

M_{N^*}	1238	1470	1900	MeV
ΔM_1	± 14	± 22	± 27	MeV
ΔM_2	± 18	± 26	± 31	MeV

Allowing for multiple scattering in traversing a beam tube of 1 mm wall thickness one finds ΔM_2 . The small influence of multiple scattering may be particular for the reaction chosen.

Using only the reconstructed particle momenta, but the original and unchanged production angles, one obtains mass resolutions which agree within the Monte-Carlo statistics with ΔM_1 .

4. DETECTORS

Four detector arrangements were presented:

- a) Small gap optical chambers in the Krienen system, by B. French.
- b) Wire chambers in the S system, by Steinberger.
- c) Optical chambers in the S system, by Steinberger.
- d) Streamer chambers in the central magnet of the H-0 system, by Hyams.

The discussion of the relative merits of different types of detectors will be reported in two parts: (1) possibility to reach the performance given by the acceptance calculations, which used a very abstract detector, (2) resolution in space and scanning possibilities.

4.1 We will proceed with a rapid description of the four detector arrangements and then summarize the discussion and comments.

- a) A layout of small gap optical spark chambers in the Krienen system was presented by B. French. The system is shown in Fig. 4; it consists of five 10-gap blocks of chambers in each downstream arm, two inside the central field, one inside the downstream analysing magnet and 2 in the field-free drift space behind; in the central field there is also one block of spark chambers of ± 1 m radial dimension, ± 1.5 m

azimuthal and ± 0.75 m in height. Photography is achieved by four cameras; one camera for each downstream arm and two cameras on top and bottom of the central field.

Discussion and Comments on a)

In the particular example presented by French, the central detector fills only $1/3$ of the radial dimension of the magnet, thereby decreasing the maximum sagitta in the central region (which is proportional to BL^2) by a factor 9; also the height is only used to one half. Krienen pointed out that for different experiments the full magnet volume could be used for particle detection by means of optical chambers. Photography is also restrictive to the direction of particles. Winter said that a detector of about the same dimension can be accommodated in the split field magnet (see p. 9, section c and Figure 6). Krienen pointed out that the French layout in the central region is very much different from that proposed by Steinberger (compare Figs. 4 and 6). Winter expressed doubt whether the hole for photography can be further increased without a rapid decrease in field, whereas Krienen was of the opinion that a hole of 2×2^2 m in a pole of 5 m diameter is acceptable for a reasonably constant field in the medium plane. Steinberger commented on the downstream detector arrangement. Photography into the downstream analysing magnet is achieved through a special slot in the iron. Consequently the system is very rigid and has low information density in a region where the multiplicity of secondaries is expected to be high. The low information density in the downstream magnet will also not allow to measure the maximum sagitta which were calculated. However, a different method of photography, an example of which is shown in Fig. 6 (downstream region) could overcome this rigidity.

b) As a proposal, Steinberger presented groups of 4 gaps of Charpak proportional chambers, with wire orientations 0° , 90° , $+45^\circ$, and -45° in the split field system. This arrangement will give the local direction of tracks similar to optical chambers, and therefore high redundancy. A total of 10^5 wires with a 2 mm spacing will approximate very well the abstract detector used in evaluating the acceptance of the system; a group of

chambers every metre in the downstream region and three groups around the central region. A typical arrangement is shown in Fig. 5. Steinberger commented on his preference for Charpak chambers; they are known to work well in high magnetic fields and have a very short sensitive time τ . Detection of particles by chambers with digital readout has several advantages. The information density can be adjusted according to the requirements and is not limited by optics. Also the orientation of planes and therefore the direction of particles is not restricted.

	<u>sensitive time</u>
Charpak chambers	100 ns
Small gap spark chamber	1 000 ns
Wide gap and streamer chamber	10 000 ns

The short sensitive time of Charpak chambers is perhaps a useful feature in view of the large background from beam-gas interactions.

Discussion and Comments on b)

Minten pointed out that wire chambers by their high price and complexity will always result in a low density of information in the central field. They will also not detect particles emitted into the full solid angle. A better detector, at least for a survey in the central field would be a streamer chamber which is an isotropic detector (later described by Hyams).

Krienen commented on the price of Charpak's chambers and said the price of readout electronics is about 40 SFr. per wire and is not expected to decrease much. Steinberger discussed an electronics scheme which uses groups of wires in Charpak chambers as hodoscope elements for event decision. In this way much of the complication of using many scintillators in high magnetic fields (long light guides) can be avoided and the trigger possibilities remain very flexible, as they require no changes in hardware.

- c) Steinberger presented a possible layout of optical spark chambers in the split field system to demonstrate the principal feasibility in case their use would be desirable. The layout is shown in Fig. 6; it uses four cameras on the sides, two top mirrors on each downstream group to get 90° stereo views and small mirrors looking into the shadow of the vacuum pipe. About 10% of the vertical space is taken up by mirrors and lost for particle detection.
- d) Hyams presented a streamer chamber arrangement in the central field of the Hyams-O'Neill system (see Fig. 7). He referred to the SLAC experience with a 2-gap chamber, 3 m long, 2 m wide and 2 x 30 cm high which is operational. He would put 4 gaps into the central magnet, giving 120 cm height, and rearrange the pillars to give space for the feed electrodes from the outside. The medium plane between the crossing beam tubes is left free over a height corresponding to the tube diameter (15 cm). He would select 4 constraints and 2 constraints events for a survey experiment by triggering on events with $N_Y \leq 2$; this would give a class of events which is between 10^{-2} and 10^{-3} of the total. The acceptance for events with a charged multiplicity n_{CH} is $(0.50)^{n_{CH}}$ for the H-O system. This detector would also see the vertex of neutral V's. The main advantage of this scheme would however be its high information density. Considering track segments of 1 cm length as independent, one arrives at a factor 10 in density with respect to wire chambers.

Discussion and Comments on d)

Steinberger recalled the problems due to the long sensitive time, perhaps 10 μ s, in the presence of heavy background. If the circulating current is not to be limited to a small value, the high information density may even not be sufficient to separate tracks from beam-beam interactions. Gregory commented on the information density in the streamer chamber. High density is required in that part of the solid angle in which the multiplicity is high. From

Summary of the discussion on optical detectors

	H-0	K	S
Possibility of optical chambers in downstream magnets	Good	Good	Good
Fraction of field volume useful for detection	1	0.9	0.9
Possibility of optical chambers near interaction point	Excellent	Good	Medium
Fraction of field volume used for detection	0.25 of height full width	0.5 of height 0.3 of width (in French layout)	0.9 of height full width

the observation of nearly constant average transverse momentum and the observed average longitudinal momenta one could conclude that high multiplicity will occur at angles below 5° . The streamer chamber in the central field and the idea of a central field altogether may not match very well with physics. Hyams pointed out that there may well exist very central collisions producing high multiplicity events at rest in the c.m. system, and cited cosmic ray results supporting this hypothesis.

Steinberger pointed out that there is no need to observe the vertex of neutral V's as the great majority decays inside the vacuum tube at the same average transverse distance from the beam, because of their small transverse momenta. The problem is then rather to sample the decay tracks well enough to see a 'gap' L between the vertex of the V and the beam-beam collision. The error on the gap, ΔL is

$$\Delta L/L \cong \frac{10^{-2}}{\tau} \cdot \frac{m}{p_T}, (\tau \text{ in } 10^{-10} \text{ s})$$

and $\Delta L/L \cong 0.1$ can be reached for lifetimes of 0.3×10^{-10} s. Hyams pointed out that in a system using the standard vacuum pipe a reasonable fraction of the neutral V's would decay outside the tube.

4.2 Space Resolution and Scanning Possibilities

Experimentally observed resolutions, defined as random deviations σ of sparks from particle tracks are given in the table.

Detector	System	σ	References
Small gap opt. chambers	compact	± 0.20 mm	Michelini
Wire spark chambers	1.2 mm spacing 2x0.5 m ch.	± 0.25	Rubbia
	1.0 mm spacing 1x0.5 m ch.	± 0.28 mm	Karlsruhe Gr.
Charpak ch.	2 mm spacing	± 0.7 mm	Charpak
	4-gap group	± 0.50 mm	
Streamer chamber	1 to \vec{E}	± 0.5 mm	DESY, SLAC
	11 to \vec{E}	± 1.0 mm	

For large optical systems the resolutions are predominantly due to the optics: distortions and index variations. Steinberger pointed out that the depth of focus, D , is limiting the minimum spark size, I , to

$$I = \pm \frac{D}{m \cdot f}$$

where f is the f-number of the lens, typically 10 for multi-spark events, m is the demagnification, typically 30 in the detectors described by French and Steinberger; $D = 1.5$ m in Steinberger's scheme, $D = 1.9$ m in French's scheme, giving

$$I = \pm 5 \text{ mm or } \pm 6 \text{ mm.}$$

If the circle of confusion is large, there is also a loss of light intensity. The resolution in wire chambers depends only on the wire spacing and on the mode of operation and no other external parameters and can therefore be estimated with more

reliability. Hyams agreed with this and said that the final resolutions, specially in the downstream regions, could be expected to be equal for optical and wire chambers.

French, Minten and Hyams insisted strongly on the possibility of scanning events, as their topology may be very complicated. Steinberger commented that at present there exist no scanning tables which can accommodate 4 pictures from 4 cameras. Winter pointed out that the topology of events is getting more complicated by the photography because of extra views out of the shadow of the vacuum pipe. Hyams insisted on the advantage of homogeneous magnet fields in the Hyams-O'Neill detector for the purpose of scanning.

Gregory asked if a combination of digital readout of wire chambers and the display of digital data in a topologically obvious way would not ease this problem. Winter answered that this is already a standard procedure at CERN using the display console of the CDC 3100. He reported prices for this installation given to him by Zanella (DD). A high resolution display with the possibility to interact with programmes by a light pen would cost about 100 000 SFr, the controller, which can serve 4-8 display consoles would cost about 200 000 SFr.

Summary of discussion on resolution and scanning

Detector	Resolution	Sensitive time	Scanning possibilities
Large system of small gap optical chambers	± 0.3 mm	1 μ s	4 pictures, complicated layout
Large streamer chamber	± 0.5 mm σ_{\perp} ± 1.0 mm σ_{11}	10 μ s	Good
Wire chambers	± 0.3 mm	1 μ s	Good on display
Charpak chambers	± 0.50 mm	0.1 μ s	Good on display

5. INTERFERENCE WITH ISR OPERATION

Several possibilities of interference with the ISR operation have been discussed.

1. Deformation of circulating proton orbits inside the magnet systems and compensating schemes.
2. Loss in luminosity due to field gradients and multipole fields and due to change in crossing angle.
3. Problems connected with installation and change of experiments (running procedures).
4. Possibility of a 2-stage programme.

5.1 De Raad and collaborators⁵⁾ have investigated the orbit deformations in the magnet systems. The circulating beams are matched to the ISR lattice by special compensating magnets or by the magnet system itself. The following table gives the change of crossing angle $\Delta\theta_{cr}$; the radial shift of the interaction point Δr_c and the largest radial deflection of the beams, Δr_{max} .

Orbit Deformations

	Steinberger	Hyams-O'Neill	Krienen
$\Delta\theta_{cr}$	$\pm 4.5^\circ$	0°	0°
Δr_c	6 cm	0	0
Δr_{max}	12 cm	4	6 cm

Comments on orbit deformations

The deformation in the Hyams-O'Neill system is small enough to accommodate in it the standard vacuum tube without moving it, if one uses the space normally allocated for injection. Injection and stacking would have to be done while the H-O magnet is off. The circulating beams are then shifted radially and the H-O magnets are switched on in synchronism with the compensators.

Both other systems would require special vacuum pipes which are, or can be deformed to contain the deflected beam orbits. This is technically feasible. But if the magnet is switched off the vacuum pipe and the surrounding detectors have to be moved; this is summarized below.

a) Fixed vacuum tube and detector arrangement

Magnet always on. Field proportional to ISR beam momenta: fixed ratio of momenta in both beams.

b) Flexible tube and detector arrangement

Tube shape proportional to magnet field; magnet can be switched off; upper limit to the ratio magnet field/ISR beam momentum; detectors have to move with the chamber.

If in any of the three systems one wants to operate at lower ISR momentum, but at the maximum field, only solution 2 with flexible tube is possible; in this case a precise disposition of the detectors has to be arranged for each momentum.

The flexibility of the tube (and of the detector) should be such that they allow to change experimental conditions between long blocks of running time. (See for further discussion under 5.3). If the magnet cannot be switched off without moving the vacuum tube and the detectors, it should be maintained in operation even if data collection is stopped due to the failure of any element of the detection system or for any other reason.

Therefore the whole system, including its power supplies, should have the same degree of reliability as the ISR ring magnets. It should also be possible to remove the whole system in periods of the order of days.

5.2 Field gradients and edge focusing effects of the magnet system will modify the focusing properties of the ISR. This can be compensated only partly (order of 50%).

De Raad and collaborators⁵⁾ (CERN/68/ISR/118) have calculated the residual effects and the resulting loss in luminosity $\Delta L/L$. Their results are summarized below (not taking into account effects in the compensating magnets for H-O and K)

	H-O	Steinberger	Krienen
$\frac{\Delta L}{L}$	3%	17%	22%
L_o	1	0.77* due to crossing angle	1

* If the opposite polarity is chosen
 $(\Delta \epsilon_{cr} = 4.5^\circ) L_o = 1.4.$

There was general agreement that these values would not distinguish between different magnet systems as the best luminosity which can be reached is uncertain in an even wider range.

5.3 Starting from a discussion of power cost if the magnet would be powered the whole year and the possible savings (2/3 year ISR operation and during half this time magnet operation, resulting in ~ 1 MSFr/year), some of the practical problems in mounting and modifying experiments were discussed. During periods of mounting and modification the other intersecting

regions should operate, with a minimum of loss in time.

Therefore, either the whole magnet or the detector alone has to be removed from the interaction region and transported to the preparation hall. This transport would take at least a few days. During periods of preparation and modification, the interaction region No.4 could be used for other, simple experiments.

5.4 It was emphasized that a two-stage project would leave more flexibility for later improvements. As an example, Johnsen mentioned that after some years of operation one could envisage to redesign the ring magnets adjacent to the interaction region to incorporate them into a larger orbit compensation scheme. The split field magnet could then be transformed into a single polarity of field of increased length in each arm. These considerations should be kept in mind when detailed designs are made. From the point of view of experimental use it would seem acceptable to replace the 2 downstream magnets of the split field system by compensators of reduced length and width.

6. De Raad and Resegotti have looked into a possible time-schedule for the present magnet system and have, in the light of its complexity, arrived at the following result:

During the first half of 1969 the recruitment of a project group and of the necessary supporting staff (drawing office) should be carried out. Meanwhile engineering studies would be undertaken by visitors and, on a part-time basis, by some members of the ISR Department.

The project proper would then start about mid-1969 and take somewhat less than four years, according to the following schedule:

- 1969 - Second half - General design:
- a) mechanical structures, supports, assembling, movements;
 - b) preferred shapes and sizes of flux return elements;
 - c) optimum coil size.
- Design and drawings of a 1:5 (or 1:4) scale model.
 - Order of the model.
- 1970 - Manufacturing of the model (January to October).
Preparation for model powering and measurements.
Continuation of detailed design and drawings of main magnets and compensators.
- Measurements on the model (October to December).
Preparation of tendering specifications.
- 1971 - Tendering and discussion with firms (January to April) and, simultaneously, shimming studies of the model and preparation of final drawings.
- Adjudications and Contracts (May to July).
- 1972 - Manufacturing and delivery of components.
- 1973 - Early months - Assembling and erection.

REFERENCES

1. Hyams, O'Neill, "Proposal for an analysing system of ISR reactions", 8 September, 1968.
2. Steinberger, "Suggestions for an ISR general purpose magnet", April 1968.
3. French, Krienen, Massam, Morpurgo, "A proposal for an open magnet system for the ISR experimental region", NP/Int.Report 68-5, 11.3.1968.
4. Ciapetti, Lueth, Steffen, Steinberger, "Acceptance tables for three alternative proposals for an ISR general purpose detector", NP/Int.Report 68-38, 26.11.1968.
5. Couchman, de Raad, Strolin, "Calculation of orbit perturbations", CERN-68/ISRU/118, 4.12.1968.
6. Krienen, "Review of Proposed Magnetic Analysis Systems for ISR Reactions", CERN-68/ISRU/109, 10.6.1968.

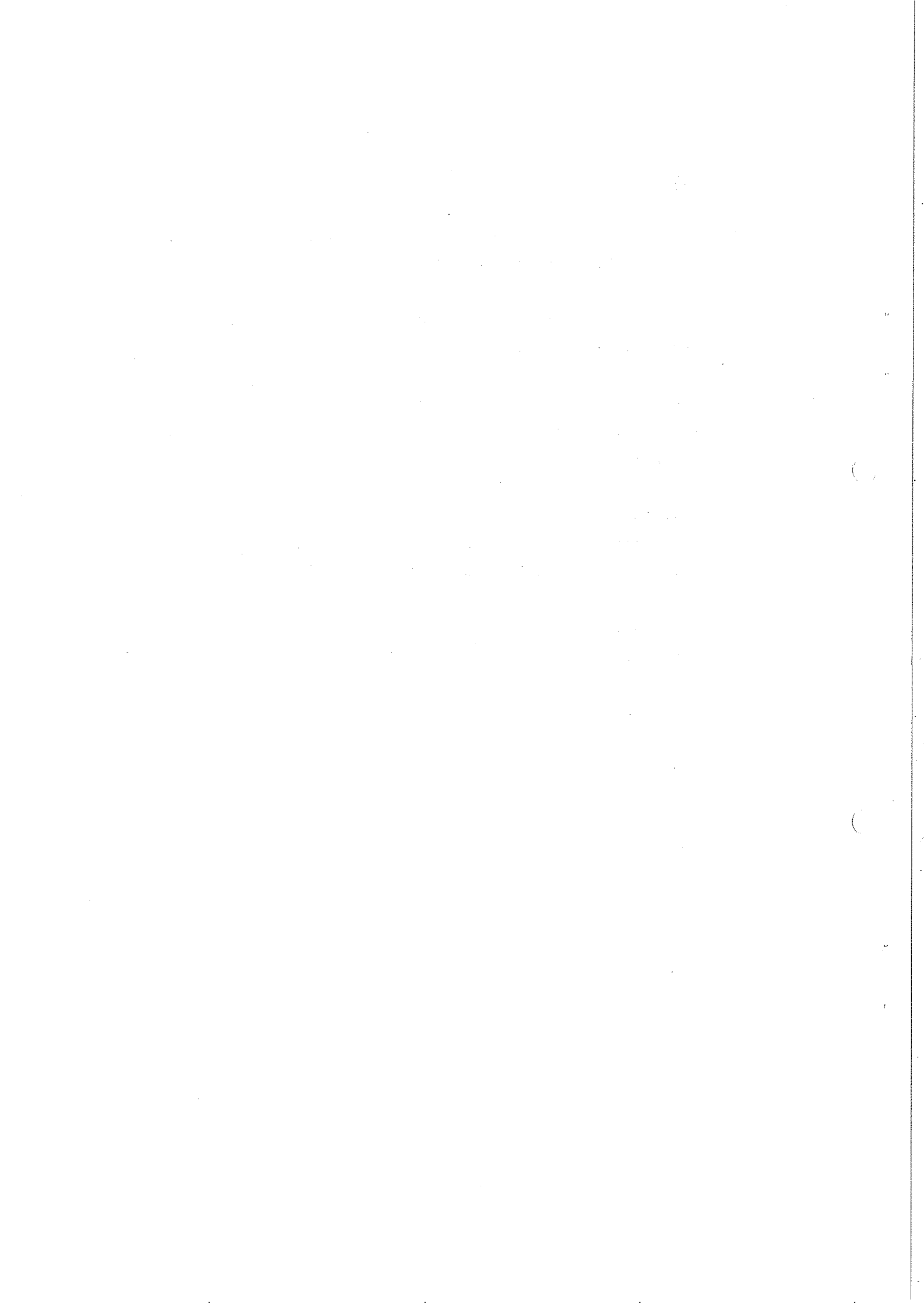


Table 1

Fraction of particles with sagitta > 2 cm, accepted by the magnet system (extracted from reference 4). Hatched areas show where this fraction is below 0.6. (Beam tube of 15 cm diameter, clearance from magnet surfaces and beam tube 5 cm).

Particles of positive charge

H - 0 *

P \ P _T	.1	.2	.3	.5	.7	1	1.5	2	3
25	0	0	0	0	0	1.0	1.0	1.0	.3
20	0	0	0	0	1.0	1.0	1.0	.7	.1
15	0	0	.3	.8	1.0	1.0	.8	.4	0
10	.3	.6	.7	1.0	1.0	.8	.2	0	0
6	1.0	.8	.8	.8	.7	.3	.2	.2	.2
4	1.0	.7	.6	.6	.3	.2	.1	.2	.1
2	.2	.4	.3	.2	.3	.7			
1	.4	.3	.3	.9	1.0	1.0			
.5	.9	1.0	1.0	1.0	.9				
$\bar{\Sigma}$.42	.42	.44	.59	.69	.75	.55	.42	.12

Average

.49

K *

P \ P _T	.1	.2	.3	.5	.7	1	1.5	2	3
25	0	0	0	0	.2	1.0	1.0	.7	.4
20	0	0	0	.2	1.0	1.0	.8	.5	.3
15	0	0	.3	1.0	1.0	1.0	.5	.4	.2
10	0	.5	.1	1.0	1.0	.6	.4	.2	0
6	.7	.8	1.0	1.0	.5	.4	.2	.7	.3
4	.8	1.0	1.0	.5	.8	.8	.9	.9	.6
2	1.0	.9	.8	.9	1.0	1.0			
1	.8	1.0	1.0	1.0	1.0	.8			
.5	1.0	1.0	1.0	1.0	.8				
$\bar{\Sigma}$.48	.58	.68	.73	.81	.93	.63	.57	.30

Average

.62

S *

P \ P _T	.1	.2	.3	.5	.7	1	1.5	2	3
25	0	0	0	0	1.0	1.0	1.0	1.0	.7
20	0	0	.4	.7	1.0	1.0	1.0	1.0	.6
15	.9	.7	.7	.8	1.0	1.0	1.0	1.0	.5
10	1.0	1.0	1.0	.9	1.0	1.0	1.0	.6	.3
6	1.0	1.0	1.0	1.0	1.0	1.0	.6	.4	.2
4	1.0	1.0	1.0	1.0	1.0	.9	.4	.3	.2
2	1.0	1.0	.9	.8	.7	.5			
1	.8	.8	1.0	.7	.5	.4			
.5	1.0	1.0	.7	.5	.4				
$\bar{\Sigma}$.75	.72	.75	.71	.84	.85	.83	.72	.42

Average

.73

* The letters H-0, K and S stand for the systems proposed by Hvams-O'Neill, Krienen and Steinberger, respectively.

TABLE

Showing the results of the tests made with the various types of material used in the construction of the various types of bridges, and the results of the tests made with the various types of material used in the construction of the various types of bridges.

TABLE I
Results of tests made with the various types of material used in the construction of the various types of bridges.

No.	Type of Material	Span (ft.)	Load (tons)	Deflection (in.)	Remarks	Date	Remarks	
							At center	At ends
1	Concrete	10	10	1.5	Good	1910		
2	Concrete	15	15	2.5	Good	1910		
3	Concrete	20	20	3.5	Good	1910		
4	Concrete	25	25	4.5	Good	1910		
5	Concrete	30	30	5.5	Good	1910		
6	Concrete	35	35	6.5	Good	1910		
7	Concrete	40	40	7.5	Good	1910		
8	Concrete	45	45	8.5	Good	1910		
9	Concrete	50	50	9.5	Good	1910		
10	Concrete	55	55	10.5	Good	1910		
11	Concrete	60	60	11.5	Good	1910		
12	Concrete	65	65	12.5	Good	1910		
13	Concrete	70	70	13.5	Good	1910		
14	Concrete	75	75	14.5	Good	1910		
15	Concrete	80	80	15.5	Good	1910		
16	Concrete	85	85	16.5	Good	1910		
17	Concrete	90	90	17.5	Good	1910		
18	Concrete	95	95	18.5	Good	1910		
19	Concrete	100	100	19.5	Good	1910		
20	Concrete	105	105	20.5	Good	1910		
21	Concrete	110	110	21.5	Good	1910		
22	Concrete	115	115	22.5	Good	1910		
23	Concrete	120	120	23.5	Good	1910		
24	Concrete	125	125	24.5	Good	1910		
25	Concrete	130	130	25.5	Good	1910		
26	Concrete	135	135	26.5	Good	1910		
27	Concrete	140	140	27.5	Good	1910		
28	Concrete	145	145	28.5	Good	1910		
29	Concrete	150	150	29.5	Good	1910		
30	Concrete	155	155	30.5	Good	1910		
31	Concrete	160	160	31.5	Good	1910		
32	Concrete	165	165	32.5	Good	1910		
33	Concrete	170	170	33.5	Good	1910		
34	Concrete	175	175	34.5	Good	1910		
35	Concrete	180	180	35.5	Good	1910		
36	Concrete	185	185	36.5	Good	1910		
37	Concrete	190	190	37.5	Good	1910		
38	Concrete	195	195	38.5	Good	1910		
39	Concrete	200	200	39.5	Good	1910		
40	Concrete	205	205	40.5	Good	1910		
41	Concrete	210	210	41.5	Good	1910		
42	Concrete	215	215	42.5	Good	1910		
43	Concrete	220	220	43.5	Good	1910		
44	Concrete	225	225	44.5	Good	1910		
45	Concrete	230	230	45.5	Good	1910		
46	Concrete	235	235	46.5	Good	1910		
47	Concrete	240	240	47.5	Good	1910		
48	Concrete	245	245	48.5	Good	1910		
49	Concrete	250	250	49.5	Good	1910		
50	Concrete	255	255	50.5	Good	1910		
51	Concrete	260	260	51.5	Good	1910		
52	Concrete	265	265	52.5	Good	1910		
53	Concrete	270	270	53.5	Good	1910		
54	Concrete	275	275	54.5	Good	1910		
55	Concrete	280	280	55.5	Good	1910		
56	Concrete	285	285	56.5	Good	1910		
57	Concrete	290	290	57.5	Good	1910		
58	Concrete	295	295	58.5	Good	1910		
59	Concrete	300	300	59.5	Good	1910		
60	Concrete	305	305	60.5	Good	1910		
61	Concrete	310	310	61.5	Good	1910		
62	Concrete	315	315	62.5	Good	1910		
63	Concrete	320	320	63.5	Good	1910		
64	Concrete	325	325	64.5	Good	1910		
65	Concrete	330	330	65.5	Good	1910		
66	Concrete	335	335	66.5	Good	1910		
67	Concrete	340	340	67.5	Good	1910		
68	Concrete	345	345	68.5	Good	1910		
69	Concrete	350	350	69.5	Good	1910		
70	Concrete	355	355	70.5	Good	1910		
71	Concrete	360	360	71.5	Good	1910		
72	Concrete	365	365	72.5	Good	1910		
73	Concrete	370	370	73.5	Good	1910		
74	Concrete	375	375	74.5	Good	1910		
75	Concrete	380	380	75.5	Good	1910		
76	Concrete	385	385	76.5	Good	1910		
77	Concrete	390	390	77.5	Good	1910		
78	Concrete	395	395	78.5	Good	1910		
79	Concrete	400	400	79.5	Good	1910		
80	Concrete	405	405	80.5	Good	1910		
81	Concrete	410	410	81.5	Good	1910		
82	Concrete	415	415	82.5	Good	1910		
83	Concrete	420	420	83.5	Good	1910		
84	Concrete	425	425	84.5	Good	1910		
85	Concrete	430	430	85.5	Good	1910		
86	Concrete	435	435	86.5	Good	1910		
87	Concrete	440	440	87.5	Good	1910		
88	Concrete	445	445	88.5	Good	1910		
89	Concrete	450	450	89.5	Good	1910		
90	Concrete	455	455	90.5	Good	1910		
91	Concrete	460	460	91.5	Good	1910		
92	Concrete	465	465	92.5	Good	1910		
93	Concrete	470	470	93.5	Good	1910		
94	Concrete	475	475	94.5	Good	1910		
95	Concrete	480	480	95.5	Good	1910		
96	Concrete	485	485	96.5	Good	1910		
97	Concrete	490	490	97.5	Good	1910		
98	Concrete	495	495	98.5	Good	1910		
99	Concrete	500	500	99.5	Good	1910		
100	Concrete	505	505	100.5	Good	1910		

* All figures given are in feet and inches unless otherwise stated.
 All figures given are in feet and inches unless otherwise stated.

Table 2

Fraction of particles with sagitta > 2 cm, accepted by the magnet system (extracted from reference 4). Hatched areas show where this fraction is below 0.6 (Beam tube of 15 cm diameter, clearance from magnet surfaces and beam tube 5 cm).

Particles of negative charge

H - 0

P \ P _T	.1	.2	.3	.5	.7	1	1.5	2	3
25	0	.3	.4	.5	.6	.7	.9	.8	.4
20	.4	.5	.6	.7	.7	.8	.9	.7	.1
15	.7	.6	.7	.7	.8	1.0	.7	.4	0
10	1.0	.8	.8	.8	.7	.7	.3	0	0
6	1.0	1.0	.8	.6	.6	.3	.2	.2	.2
4	.8	.6	.6	.5	.3	.2	.1	.2	.1
2	0	.7	.6	.4	.1	.6			
1	.8	.3	.4	.8	1.0	1.0			
.5	1.0	.9	.9	1.0	.9				
$\bar{\Sigma}$.53	.63	.64	.67	.63	.66	.52	.38	.13

Average

.53

K

P \ P _T	.1	.2	.3	.5	.7	1	1.5	2	3
25	0	0	0	.5	.6	.8	1.0	.7	.4
20	0	0	.4	.6	.7	1.0	.8	.5	.3
15	.1	.5	.6	.7	1.0	1.0	.6	.4	.2
10	.6	.7	.7	1.0	1.0	.6	.4	.2	0
6	1.0	1.0	1.0	1.0	.5	.5	.6	.7	.4
4	1.0	1.0	1.0	.8	.9	.9	.9	1.0	.6
2	1.0	1.0	1.0	1.0	1.0	1.0			
1	1.0	1.0	1.0	1.0	1.0	.8			
.5	1.0	1.0	1.0	1.0	.8				
$\bar{\Sigma}$.63	.69	.74	.84	.83	.82	.72	.58	.32

Average

.69

S

P \ P _T	.1	.2	.3	.5	.7	1	1.5	2	3
25	0	.2	.4	.9	1.0	1.0	.9	.9	.7
20	1.0	1.0	1.0	1.0	1.0	1.0	.9	1.0	.6
15	1.0	1.0	1.0	1.0	1.0	1.0	1.0	1.0	.5
10	1.0	1.0	1.0	1.0	1.0	1.0	1.0	.7	.4
6	1.0	1.0	1.0	1.0	1.0	1.0	.7	.5	.3
4	1.0	1.0	1.0	1.0	1.0	.9	.5	.4	.2
2	1.0	1.0	1.0	1.0	.8	.4			
1	1.0	1.0	1.0	.6	.5	.4			
.5	1.0	1.0	.7	.4	.4				
$\bar{\Sigma}$.89	.91	.90	.88	.86	.84	.83	.58	.45

Average

.79

1. The first part of the document is a list of names and their corresponding numbers.

List of names and numbers

1	2	3	4	5	6	7	8	9	10
11	12	13	14	15	16	17	18	19	20
21	22	23	24	25	26	27	28	29	30
31	32	33	34	35	36	37	38	39	40
41	42	43	44	45	46	47	48	49	50
51	52	53	54	55	56	57	58	59	60
61	62	63	64	65	66	67	68	69	70
71	72	73	74	75	76	77	78	79	80
81	82	83	84	85	86	87	88	89	90
91	92	93	94	95	96	97	98	99	100

11
 12

1	2	3	4	5	6	7	8	9	10
11	12	13	14	15	16	17	18	19	20
21	22	23	24	25	26	27	28	29	30
31	32	33	34	35	36	37	38	39	40
41	42	43	44	45	46	47	48	49	50
51	52	53	54	55	56	57	58	59	60
61	62	63	64	65	66	67	68	69	70
71	72	73	74	75	76	77	78	79	80
81	82	83	84	85	86	87	88	89	90
91	92	93	94	95	96	97	98	99	100

11
 12

1	2	3	4	5	6	7	8	9	10
11	12	13	14	15	16	17	18	19	20
21	22	23	24	25	26	27	28	29	30
31	32	33	34	35	36	37	38	39	40
41	42	43	44	45	46	47	48	49	50
51	52	53	54	55	56	57	58	59	60
61	62	63	64	65	66	67	68	69	70
71	72	73	74	75	76	77	78	79	80
81	82	83	84	85	86	87	88	89	90
91	92	93	94	95	96	97	98	99	100

11
 12

Table 3

Fraction of particles with sagitta > 2 cm accepted by the magnet systems. Hatched areas show where this fraction is below 0.6. (Beam tube of 6 cm diameter, no clearance from the beam tube, but 5 cm clearance from magnet surfaces).

Positive particles

H - 0

P \ P _T	0	.1	.2	.3	.4	.5	.6	.7	.8	.9	1
25	0	0	0	0	.37	.47	.63	.95	1	1	1
20	0	0	0	.26	.74	1	1	1	1	1	1
15	0	.58	.74	1	1	1	1	1	1	1	1
10	1	1	1	1	1	1	1	1	1	.84	.79
6	1	1	1	.95	.89	.79	.79	.84	.68	.53	.33
4	1	1	.79	.74	.84	.89	.53	.42	.37	.37	.37
2	0	.79	.89	.53	.89	.95	.95	1	1	1	1
1	0	.89	1	1	1	1	1	1	1	1	1
Σ	.37	.66	.68	.68	.84	.89	.86	.90	.88	.84	.84

Average: .768

K

P \ P _T	0	.1	.2	.3	.4	.5	.6	.7	.8	.9	1
25	0	0	1	1	1	1	1	1	1	1	1
20	0	.37	1	1	1	1	1	1	1	1	1
15	0	.68	1	1	1	1	1	1	1	1	1
10	1	.84	1	1	1	1	1	1	1	.74	.63
6	1	1	1	1	1	1	1	1	1	1	1
4	1	1	1	1	1	1	1	1	.95	.95	.95
2	1	1	1	.95	.95	1	1	1	1	1	1
1	0	.95	1	1	1	1	1	1	1	1	.84
Σ	.50	.74	1	.99	.99	1	1	1	.99	.97	.93

Average: .920

S

P \ P _T	0	.1	.2	.3	.4	.5	.6	.7	.8	.9	1
25	0	0	1	1	1	1	1	1	1	1	1
20	1	.84	.79	1	1	1	1	1	1	1	1
15	1	1	1	1	1	1	1	1	1	1	1
10	1	1	1	1	1	1	1	1	1	1	1
6	1	1	1	1	1	1	1	1	1	1	1
4	1	1	1	1	1	1	1	1	1	1	.75
2	1	1	1	1	1	.95	.95	1	.84	.68	.63
1	1	1	.95	1	1	1	.63	.53	.47	.42	.37
Σ	.87	.85	.97	1	1	.99	.95	.94	.91	.89	.87

Average: .932

1. The first part of the document is a list of names and their corresponding addresses. The names are listed in the first column, and the addresses are listed in the second column. The names are:

Name	Address
John Doe	123 Main St, New York, NY 10001
Jane Smith	456 Elm St, Los Angeles, CA 90001
Bob Johnson	789 Oak St, Chicago, IL 60601
Alice Brown	101 Pine St, San Francisco, CA 94101
Charlie White	202 Cedar St, Houston, TX 77001
Diana Green	303 Birch St, Phoenix, AZ 85001
Frank Black	404 Spruce St, Philadelphia, PA 19101
Grace King	505 Willow St, San Diego, CA 92101
Henry Lee	606 Ash St, Dallas, TX 75201
Ivy Hill	707 Sycamore St, Austin, TX 78701
Jack Adams	808 Magnolia St, Fort Worth, TX 76101
Karen Baker	909 Dogwood St, Columbus, GA 31901
Leo Clark	1010 Redwood St, Sacramento, CA 95811
Mia Evans	1111 Cypress St, San Jose, CA 95101
Noah Foster	1212 Juniper St, Denver, CO 80201
Olivia Garcia	1313 Fir St, Portland, OR 97201
Peter Hall	1414 Hemlock St, Seattle, WA 98101
Quinn Ives	1515 Larch St, Minneapolis, MN 55401
Rachel King	1616 Alder St, St. Paul, MN 55101
Samuel Lee	1717 Spruce St, Des Moines, IA 50301
Tina Miller	1818 Fir St, Omaha, NE 68101
Uma Nunez	1919 Cedar St, Lincoln, NE 68501
Victor Ortiz	2020 Birch St, Kansas City, MO 64101
Wendy Parker	2121 Willow St, St. Louis, MO 63101
Xavier Quinn	2222 Ash St, St. Petersburg, FL 33701
Yara Ramirez	2323 Sycamore St, Tampa, FL 33601
Zoe Roberts	2424 Magnolia St, Orlando, FL 32801

2. The second part of the document is a list of names and their corresponding addresses. The names are listed in the first column, and the addresses are listed in the second column. The names are:

Name	Address
John Doe	123 Main St, New York, NY 10001
Jane Smith	456 Elm St, Los Angeles, CA 90001
Bob Johnson	789 Oak St, Chicago, IL 60601
Alice Brown	101 Pine St, San Francisco, CA 94101
Charlie White	202 Cedar St, Houston, TX 77001
Diana Green	303 Birch St, Phoenix, AZ 85001
Frank Black	404 Spruce St, Philadelphia, PA 19101
Grace King	505 Willow St, San Diego, CA 92101
Henry Lee	606 Ash St, Dallas, TX 75201
Ivy Hill	707 Sycamore St, Austin, TX 78701
Jack Adams	808 Magnolia St, Fort Worth, TX 76101
Karen Baker	909 Dogwood St, Columbus, GA 31901
Leo Clark	1010 Redwood St, Sacramento, CA 95811
Mia Evans	1111 Cypress St, San Jose, CA 95101
Noah Foster	1212 Juniper St, Denver, CO 80201
Olivia Garcia	1313 Fir St, Portland, OR 97201
Peter Hall	1414 Hemlock St, Seattle, WA 98101
Quinn Ives	1515 Larch St, Minneapolis, MN 55401
Rachel King	1616 Alder St, St. Paul, MN 55101
Samuel Lee	1717 Spruce St, Des Moines, IA 50301
Tina Miller	1818 Fir St, Omaha, NE 68101
Uma Nunez	1919 Cedar St, Lincoln, NE 68501
Victor Ortiz	2020 Birch St, Kansas City, MO 64101
Wendy Parker	2121 Willow St, St. Louis, MO 63101
Xavier Quinn	2222 Ash St, St. Petersburg, FL 33701
Yara Ramirez	2323 Sycamore St, Tampa, FL 33601
Zoe Roberts	2424 Magnolia St, Orlando, FL 32801

3. The third part of the document is a list of names and their corresponding addresses. The names are listed in the first column, and the addresses are listed in the second column. The names are:

Name	Address
John Doe	123 Main St, New York, NY 10001
Jane Smith	456 Elm St, Los Angeles, CA 90001
Bob Johnson	789 Oak St, Chicago, IL 60601
Alice Brown	101 Pine St, San Francisco, CA 94101
Charlie White	202 Cedar St, Houston, TX 77001
Diana Green	303 Birch St, Phoenix, AZ 85001
Frank Black	404 Spruce St, Philadelphia, PA 19101
Grace King	505 Willow St, San Diego, CA 92101
Henry Lee	606 Ash St, Dallas, TX 75201
Ivy Hill	707 Sycamore St, Austin, TX 78701
Jack Adams	808 Magnolia St, Fort Worth, TX 76101
Karen Baker	909 Dogwood St, Columbus, GA 31901
Leo Clark	1010 Redwood St, Sacramento, CA 95811
Mia Evans	1111 Cypress St, San Jose, CA 95101
Noah Foster	1212 Juniper St, Denver, CO 80201
Olivia Garcia	1313 Fir St, Portland, OR 97201
Peter Hall	1414 Hemlock St, Seattle, WA 98101
Quinn Ives	1515 Larch St, Minneapolis, MN 55401
Rachel King	1616 Alder St, St. Paul, MN 55101
Samuel Lee	1717 Spruce St, Des Moines, IA 50301
Tina Miller	1818 Fir St, Omaha, NE 68101
Uma Nunez	1919 Cedar St, Lincoln, NE 68501
Victor Ortiz	2020 Birch St, Kansas City, MO 64101
Wendy Parker	2121 Willow St, St. Louis, MO 63101
Xavier Quinn	2222 Ash St, St. Petersburg, FL 33701
Yara Ramirez	2323 Sycamore St, Tampa, FL 33601
Zoe Roberts	2424 Magnolia St, Orlando, FL 32801

4. The fourth part of the document is a list of names and their corresponding addresses. The names are listed in the first column, and the addresses are listed in the second column. The names are:

Table 4

Fraction of particles with dagitta > 2 cm accepted by the magnet systems. Hatched areas show where this fraction is below 0.6. (Beam tube of 6 cm diameter, no clearance from the beam tube, but 5 cm clearance from magnet surfaces.)

Negative Particles

H - 0

P \ P _T	0	.1	.2	.3	.4	.5	.6	.7	.8	.9	1
25	0	0	.32	.37	.68	.74	.79	.84	.84	.84	.89
20	1	.84	.68	.68	.74	.79	.84	.84	.89	.89	.95
15	1	1	1	1	.95	.89	.89	1	1	1	1
10	1	1	1	1	.95	.95	1	.84	.79	.74	.68
6	1	1	1	1	1	1	1	1	.84	.63	.63
4	1	1	1	1	1	1	.63	.53	.47	.37	.32
2	1	.84	1	.84	1	1	.95	.95	1	1	1
1	1	1	.95	.	1	1	1	1	1	1	1
Σ	.87	.84	.87	.86	.92	.92	.94	.87	.85	.81	.81

Average: .870

K

P \ P _T	0	.1	.2	.3	.4	.5	.6	.7	.8	.9	1
25	1	1	1	1	.89	.84	.89	1	1	1	1
20	1	1	1	1	.89	.95	1	1	1	1	1
15	1	1	1	1	1	1	1	1	1	1	1
10	1	1	1	.95	1	1	1	1	1	.74	.63
6	1	1	1	1	1	1	1	1	1	1	1
4	1	1	1	1	1	1	1	1	1	1	1
2	1	1	1	1	1	1	1	1	1	1	1
1	1	1	1	1	1	1	1	1	1	1	.84
Σ	1	1	1	.99	.97	.97	.99	1	1	.97	.93

Average: .985

S

P \ P _T	0	.1	.2	.3	.4	.5	.6	.7	.8	.9	1
25	1	1	1	1	1	1	1	1	1	1	1
20	1	1	1	1	1	1	1	1	1	1	1
15	1	1	1	1	1	1	1	1	1	1	1
10	1	1	1	1	1	1	1	1	1	1	1
6	1	1	1	1	1	1	1	1	1	1	1
4	1	1	1	1	1	1	1	1	1	1	1
2	1	1	1	1	1	1	1	1	.79	.68	.58
1	1	1	1	1	1	.79	.58	.47	.42	.37	.37
Σ	1	1	1	1	1	.97	.95	.93	.90	.88	.89

Average: .948

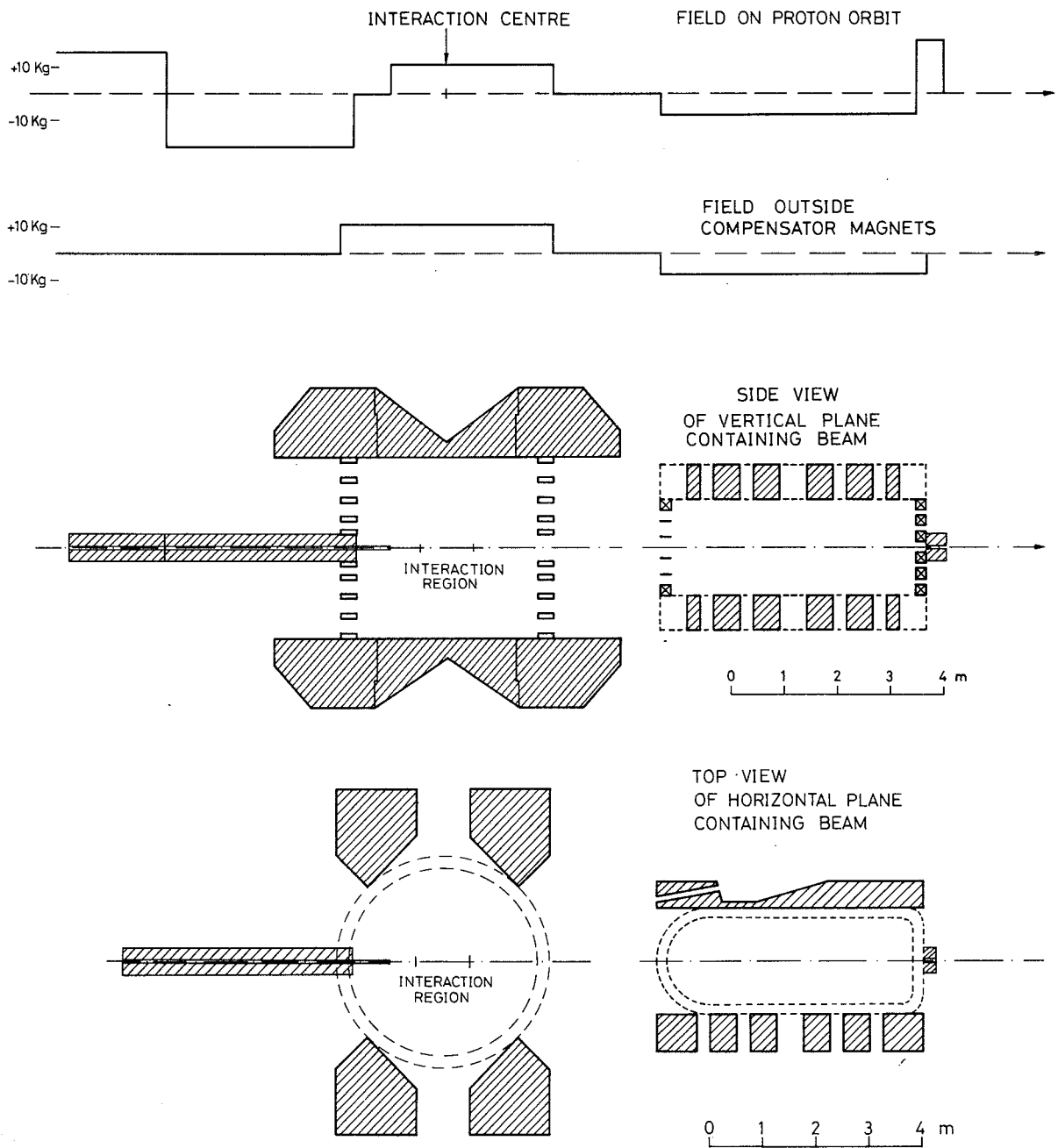


Fig. 1

Hyams - O'Neill Proposal

THESE DOCUMENTS ARE LOANED

TO THE NATIONAL ARCHIVES



RECEIVED

DATE: 10/10/1963

FROM: [illegible]

[illegible text]

[illegible text]

[illegible text]

[illegible text]

[illegible text]

10/10/63

10/10/63

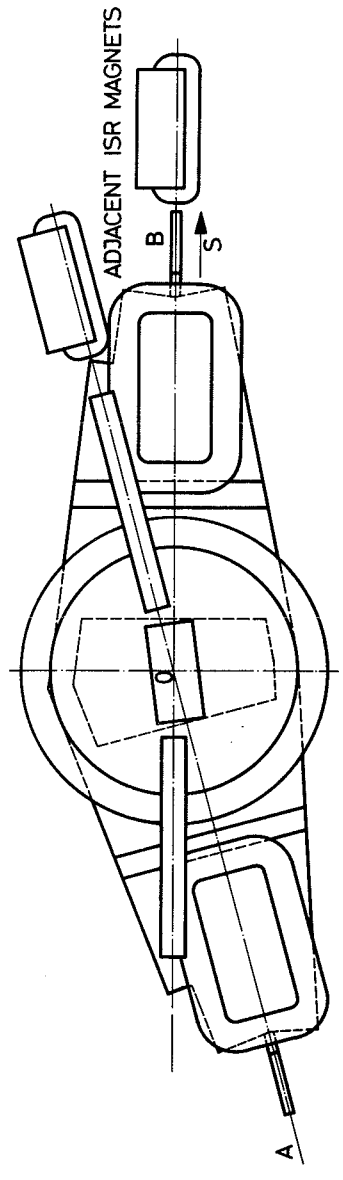
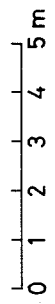
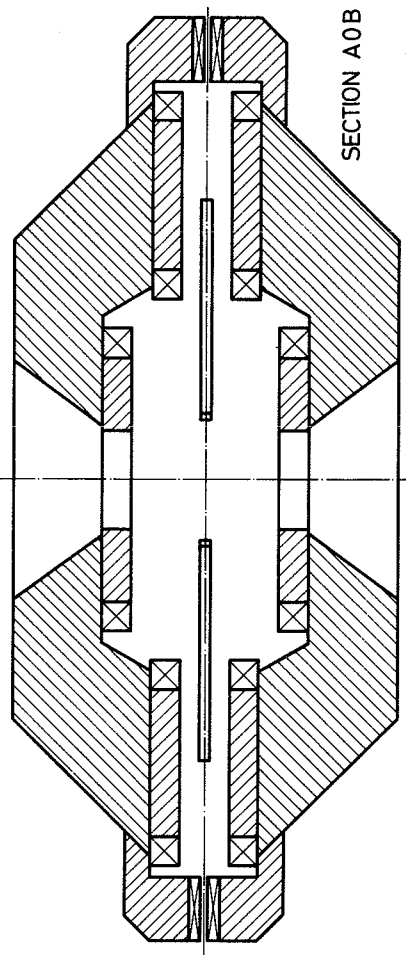
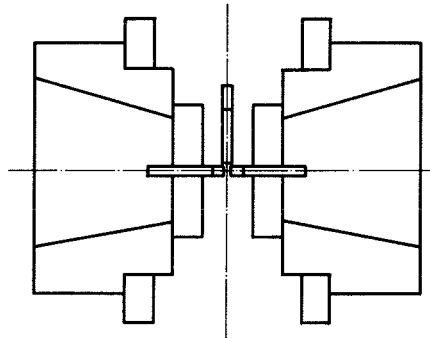
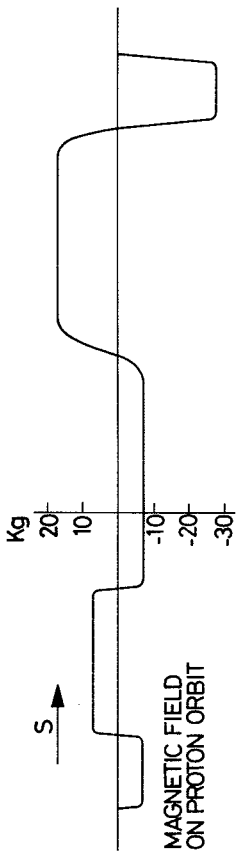
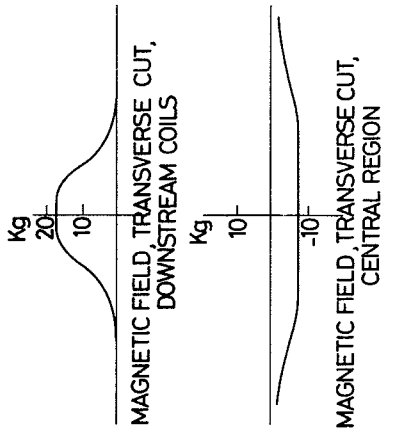
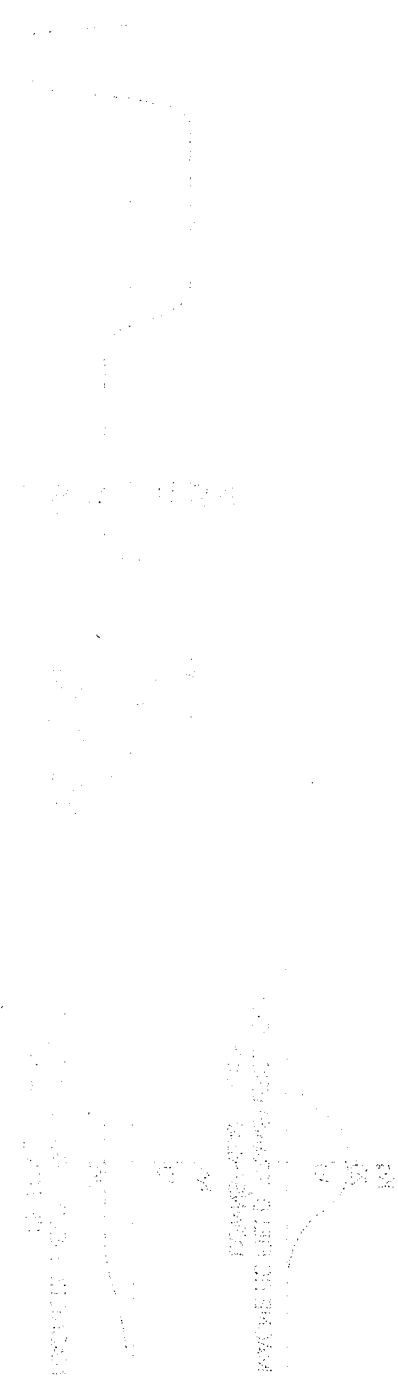


Fig. 2
Krienen Proposal

1942
1943



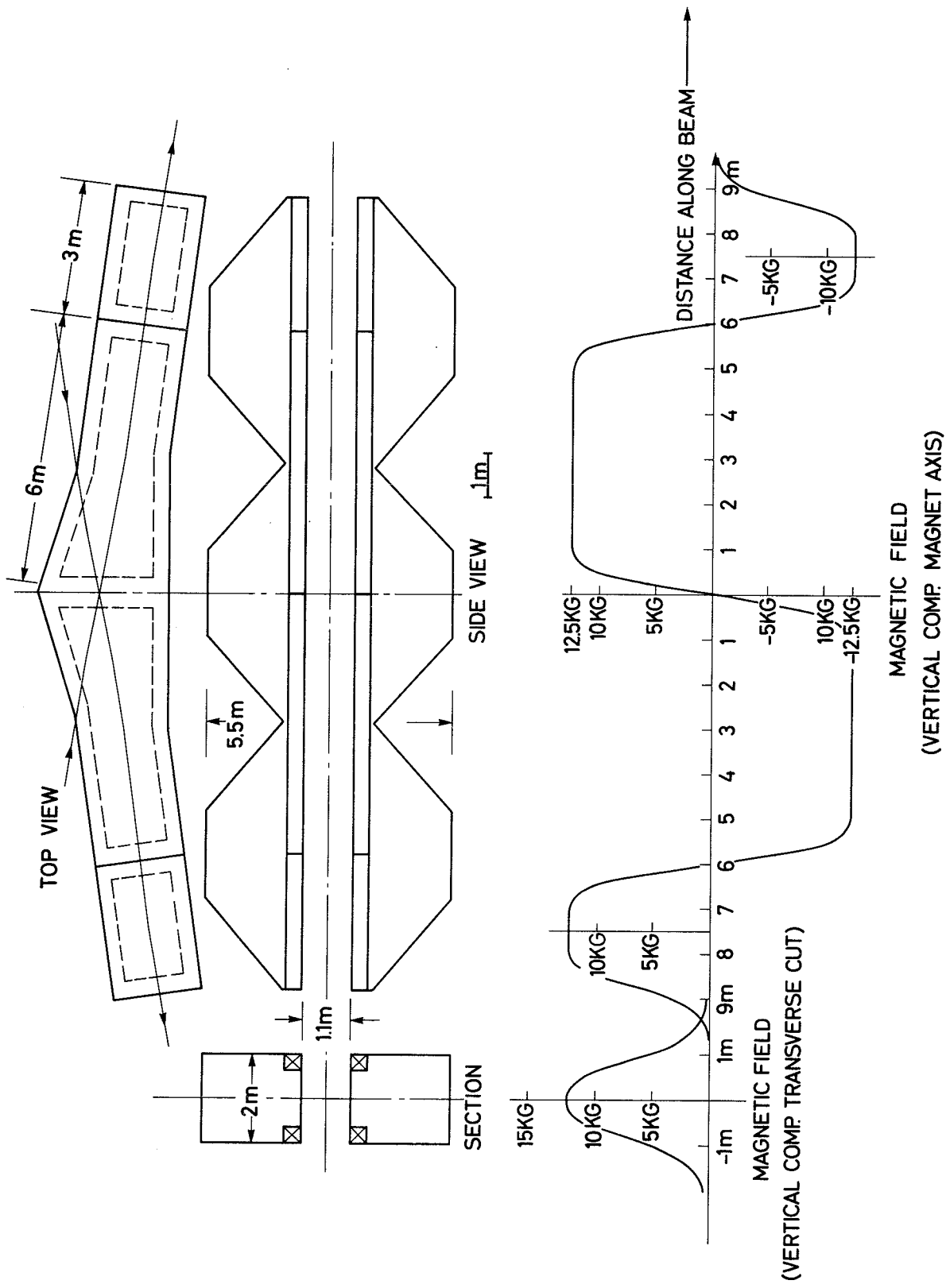


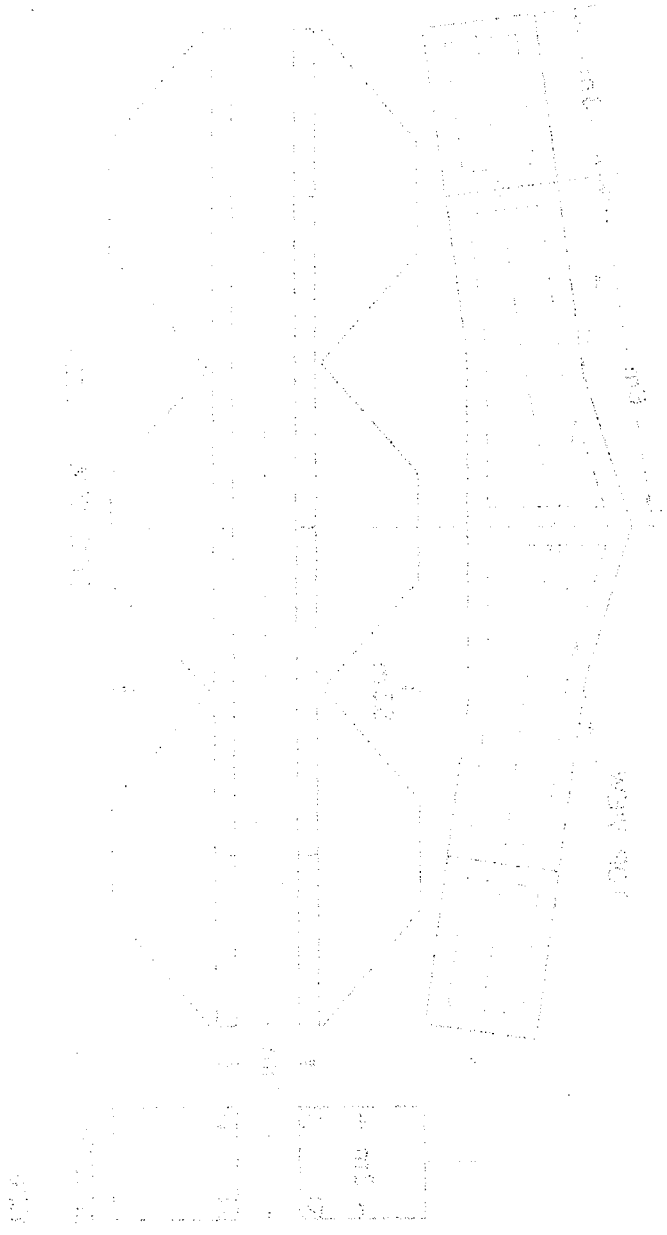
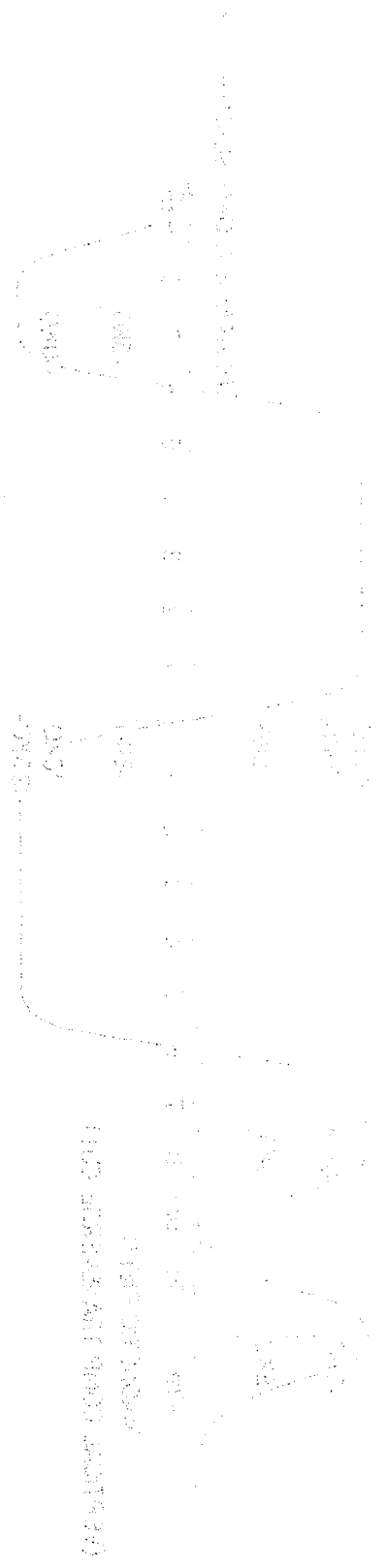
Fig. 3

Steinberger Proposal

21/05/2024 (John)

AP 1

APPROXIMATE BOUNDING BOX
FOR THE BUILDING



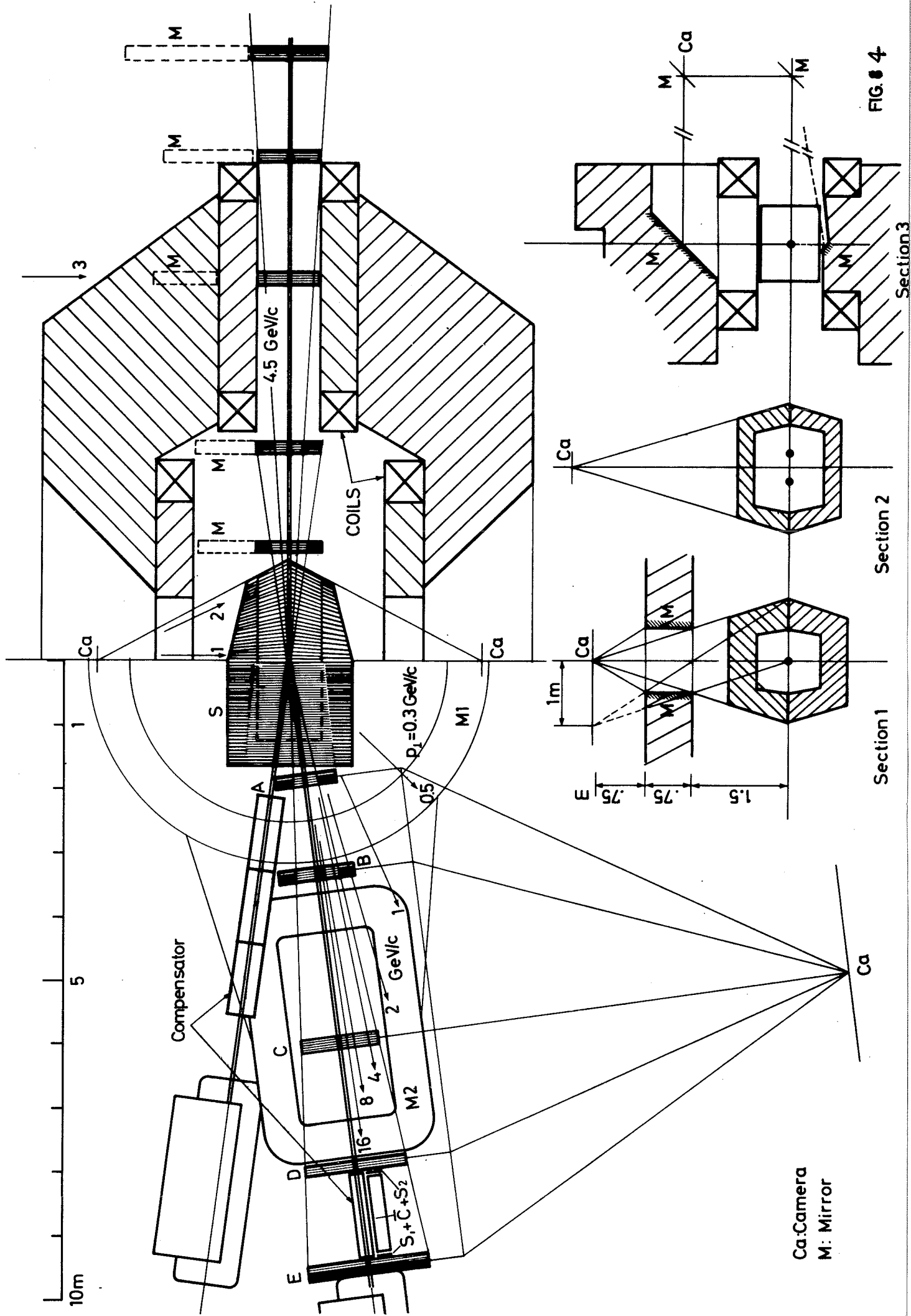
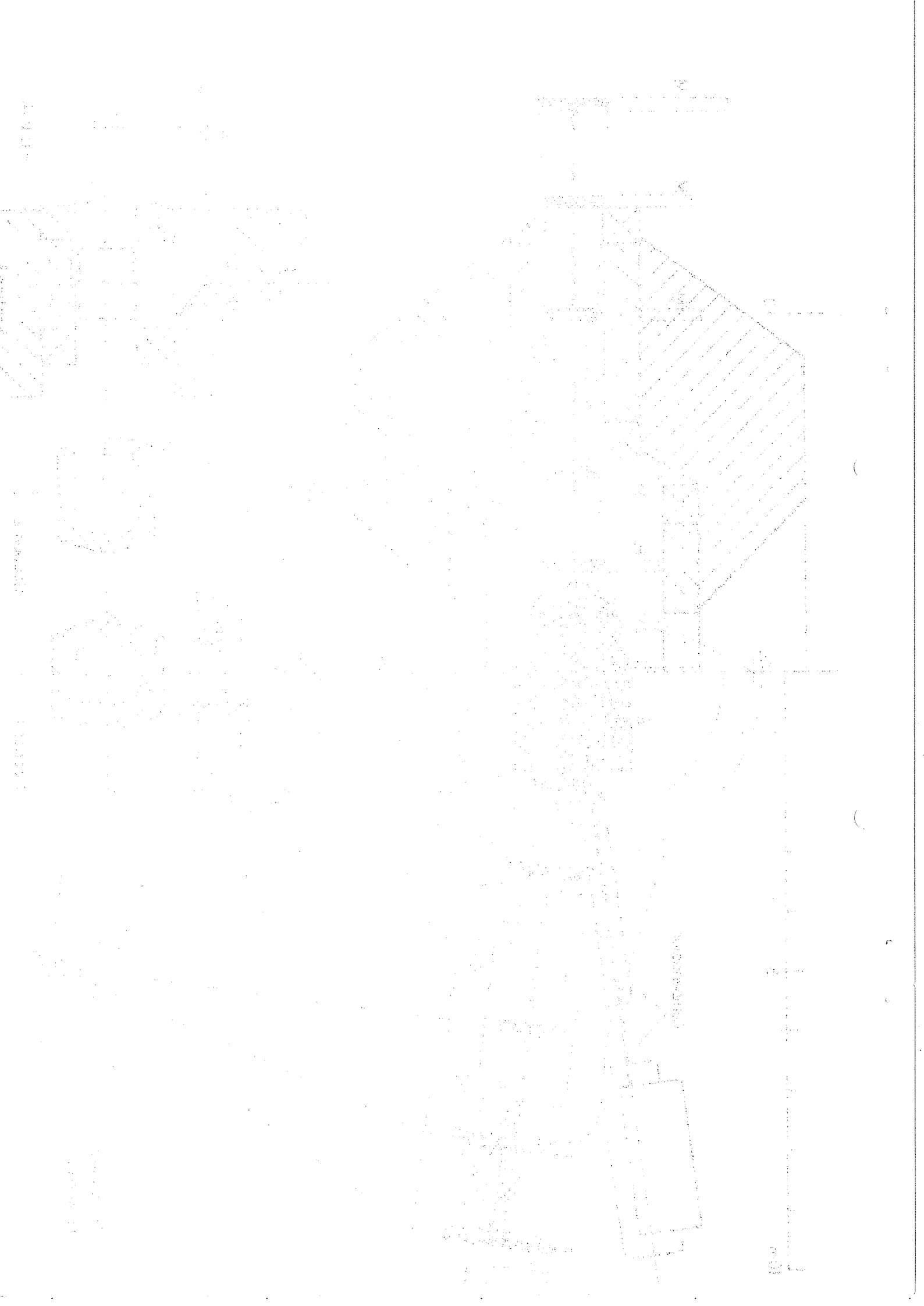


FIG. 4



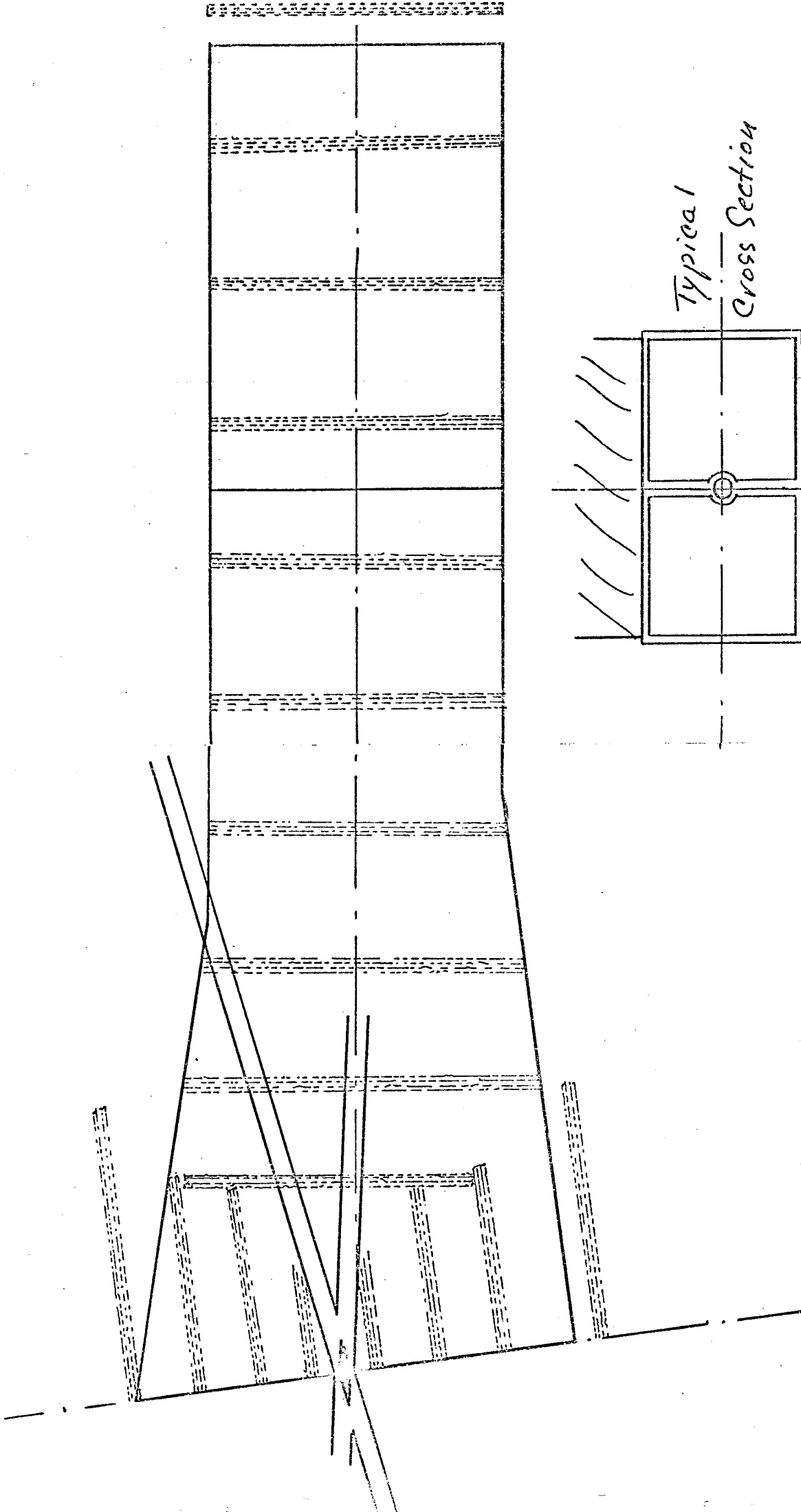
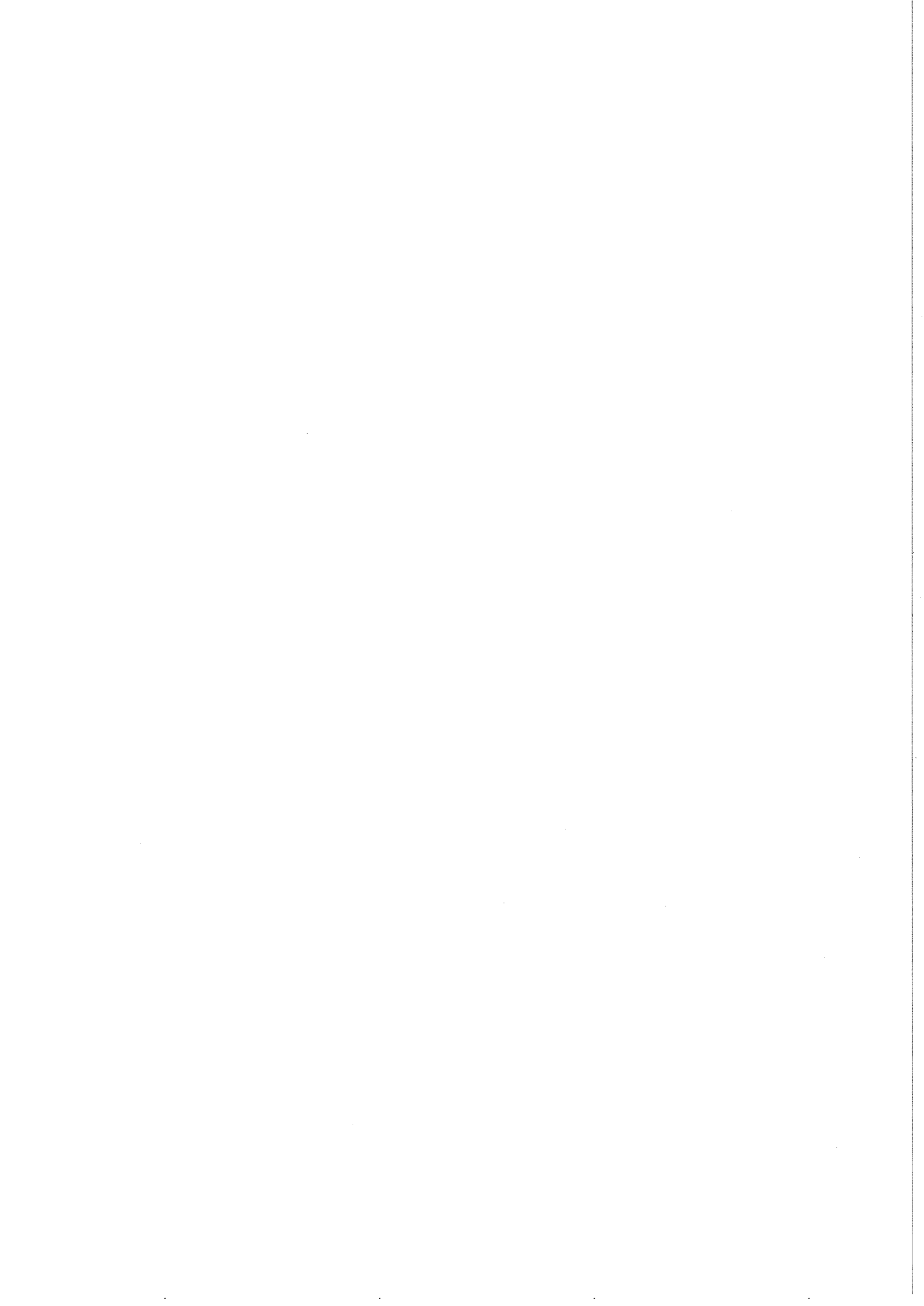
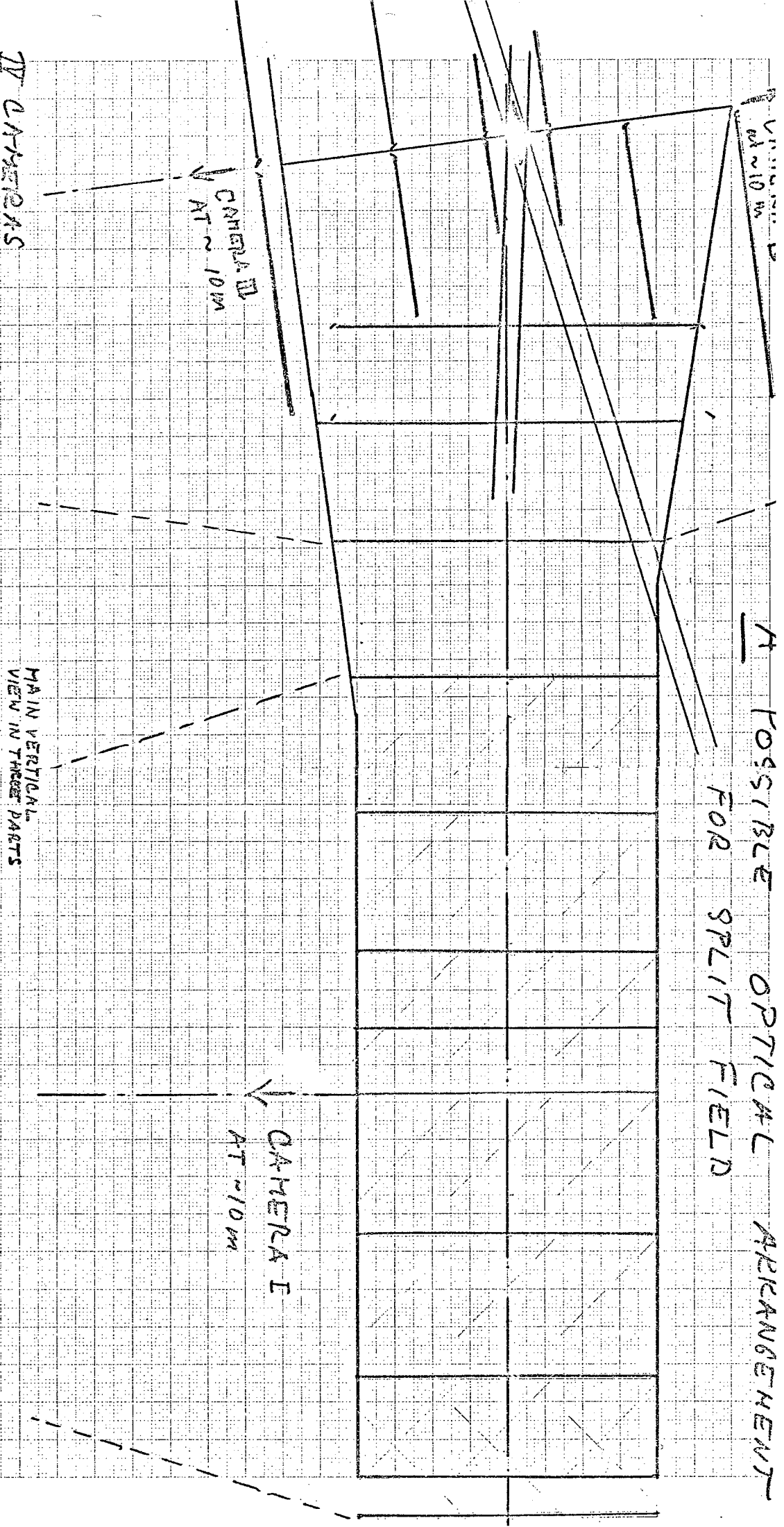


FIG. 5



A POSSIBLE OPTICAL ARRANGEMENT FOR SPLIT FIELD



IV CAMERAS
 EACH TAKES ~ 1/5000
 OF 35MM FILM.
 MAGNIFICATION 1:30
 EXTRA
 CROSS OF FIDUCIAL MARKS
 VOLUME DUE TO OPTICS:
 VERTICAL ~ 5cm in 100cm.
 AT 900 base ~ ± 3°.

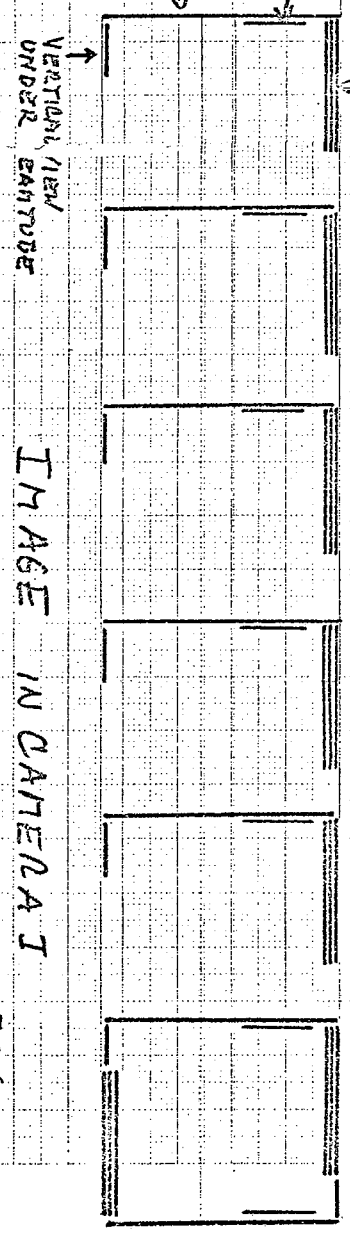
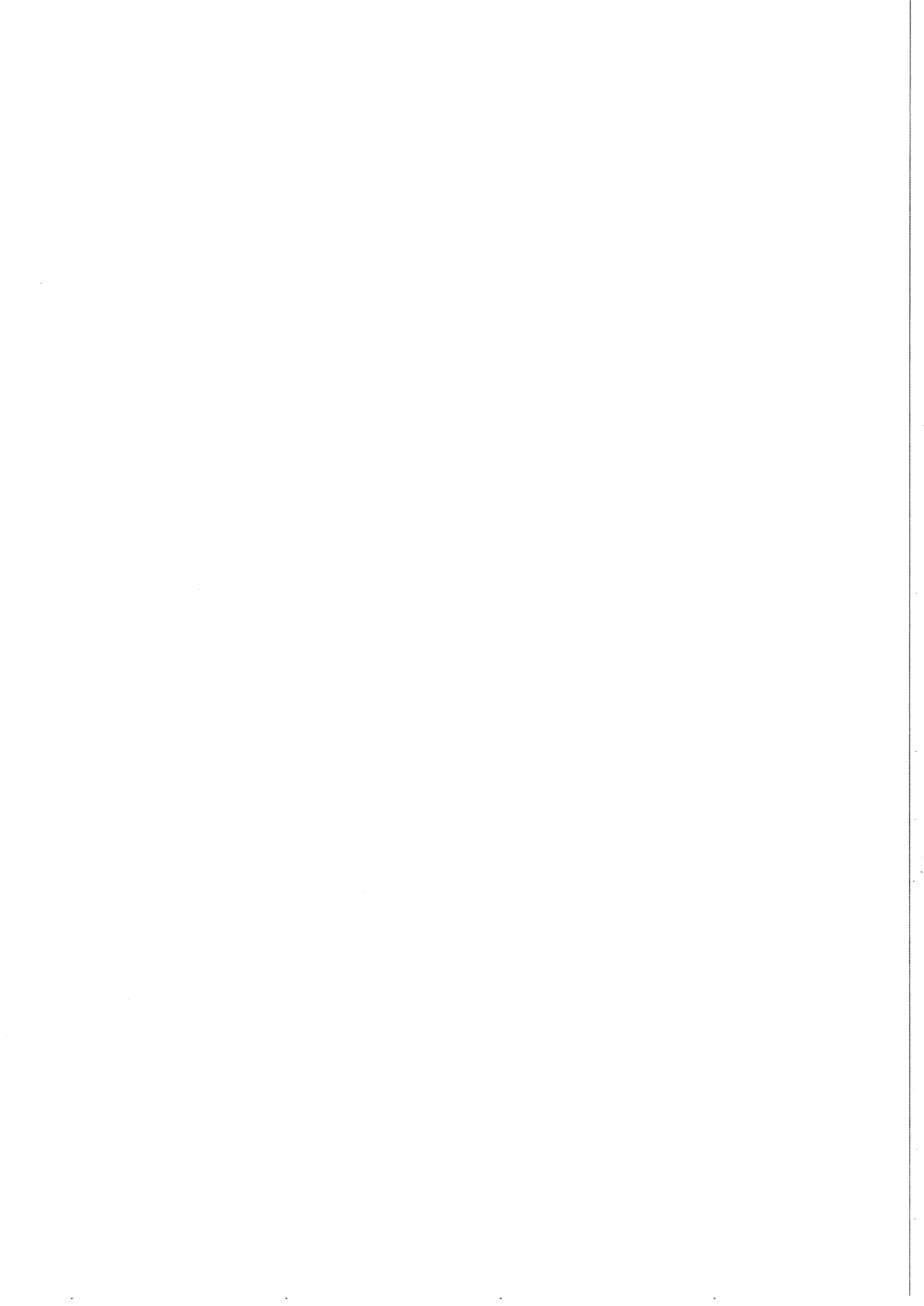
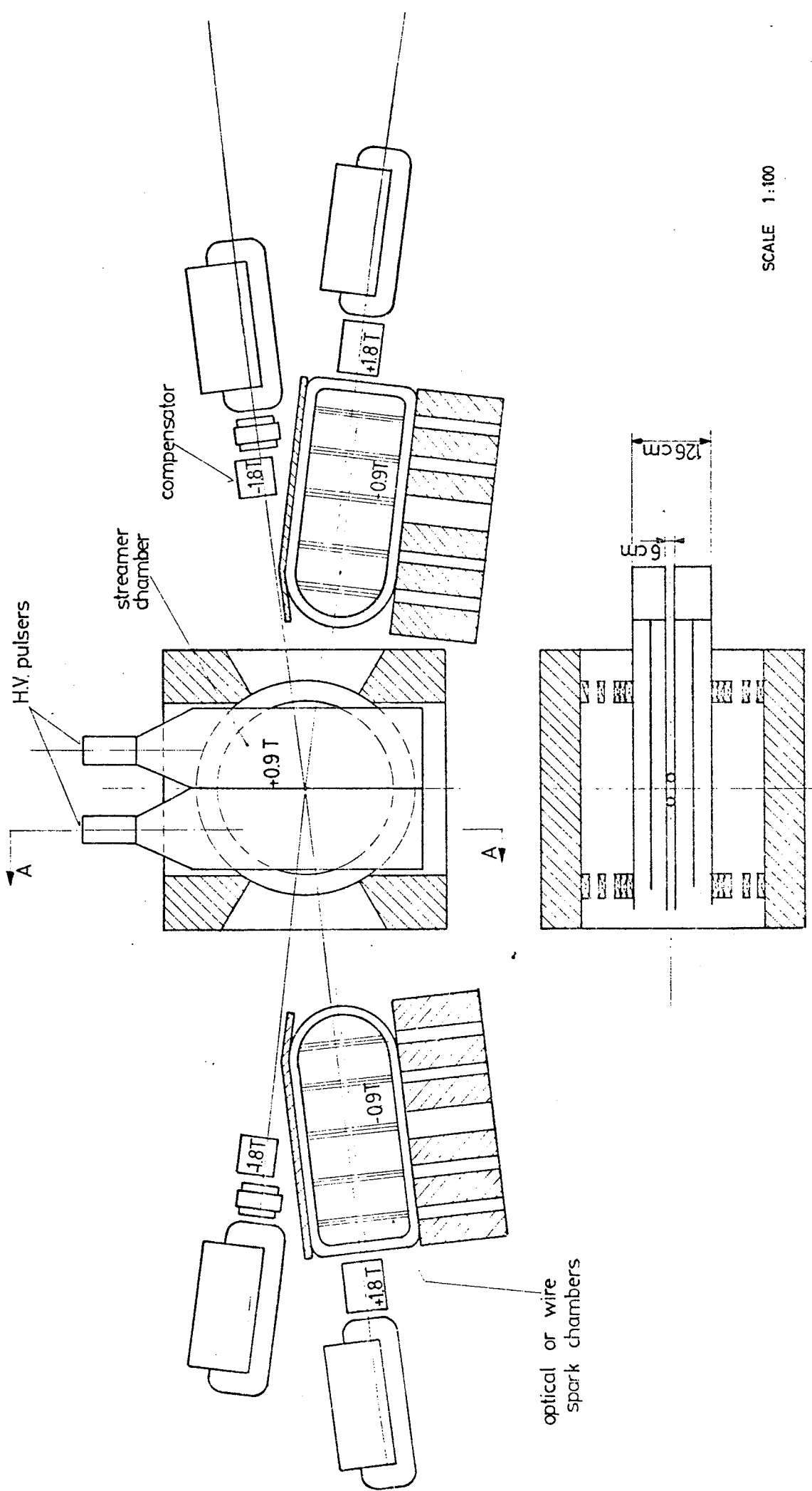


FIG. 6



HYAMS O'NEILL MAGNET SYSTEM

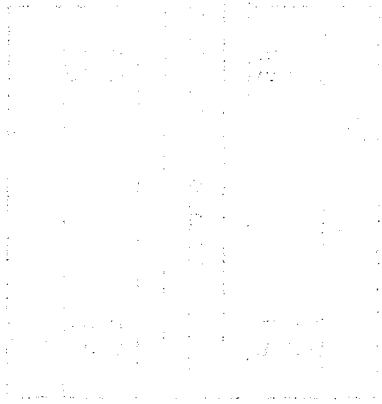
(Crossing Point has moved right by 50 cm , all compensators shown)



SCALE 1:100

FIG. 7

SECTION AA



1001

1001

1001

1001